

Estimating vegetation height using L and X band synthetic aperture radar images for effective river management

Syota Sasaki¹, Ariyo Kanno¹, and Yoshiyuki Imamura¹

¹Yamaguchi University, 2-28-4, Tokiwadai, Yamaguchi 755-8611, Japan,

Email: s-sasaki@yamaguchi-u.jp

KEY WORDS: synthetic aperture radar, vegetation monitoring, drone aerial shooting, river management, estimation of vegetation height

ABSTRACT: We proposed a method to estimate vegetation height using two synthetic aperture radar images with two different wave lengths. While L band microwave penetrates vegetation, X band microwave is scattered by vegetation. Using the different reflection-scattering properties of L and X band microwaves, we estimated vegetation heights on a riverbank. We used the vegetation heights measured by drone aerial shooting to verify the estimated heights, and the mean and standard deviation of the relative errors by the proposed method are -15.6 %, 17.0 %, respectively.

1. INTRODUCTION

1.1 Research background

Lush vegetation blocks river flow and causes riverbank erosion in Japan (Shige-eda et al. 2006, Shimizu, Y. et al. 2006, Okamoto, T. et al. 2013). Managing vegetation in riverine areas is critical to reduce flood disasters. At the first-class rivers in Japan, vegetation is monitored once in five years. However, the five-year interval is too long for effective vegetation management because vegetation grows and the state of riverine areas changes for the five years. After vegetation grew, flood risk increases and it needs more cost to cut and dispose vegetation. Thus, frequent, wide, and inexpensive vegetation monitoring using satellite remote sensing technology is expected for effective and efficient vegetation management in riverine areas.

1.2 Objectives

Satellite remote sensing has the advantages of high frequent and wide observation for vegetation monitoring. While synthetic aperture radar (SAR) satellite technology is used for observation of vegetation that grows densely and broadly, such as tropical rainforest (JAXA 2016), there are few examples of applying the technology to vegetation in a Japanese river (Partama et al. 2016). It is because vegetation areas in Japanese rivers are smaller and more scattered than those of continental rivers.

In this study, we proposed a method to estimate vegetation heights using two SAR satellite images with different wavelengths. Accuracy of the method is verified by comparing with measured heights by drone aerial shooting. It is expected that the proposed vegetation monitoring by SAR contributes to more frequent monitoring and effective river management.

This paper reports a part of a series of studies. The first findings of the studies are published in Japanese with peer review (Sasaki et al. 2017). This paper includes the first findings with some additional discussions.

1.3 Study area

We applied the proposed method to the Saba River in Yamaguchi Prefecture, Japan (Figure 1). Although the river is designated as a first-class river by the Ministry of Land, Infrastructure, Transport and Tourism (MLIT), Japan, and the MLIT monitors the river intensively, the river is relatively small river (river basin area 460 km², length 172.7 km).. In that reason, we selected the Saba River as the study area to verify whether the proposed method is applicable to small rivers with poor monitoring data or not. A map of Japan and the location of the Saba River are shown in Figure 1.

Japanese timber bamboo is a dominant tree at riverine areas in western Japan including the Saba River (Sanuki et al. 2010). Thus, we applied the proposed method to Japanese timber bamboo in the river.



Figure 1: Map of Japan and location of the Saba River.

2. METHOD

2.1 Difference of reflection-scattering properties between L and X band microwaves

Reflection, scattering, and diffraction occur when electromagnetic wave encounters objects. When wave length is same or smaller than a size of an object, reflection and scattering are dominant. Diffraction is dominant when wave length is larger than a size of an object.

Microwaves are categorized into several bands by wave lengths as shown in Figure 2. The wave lengths of L and X band microwaves are approximately 15-30, 2.4-3.8 cm, respectively. Since the wavelength of X band microwave is smaller than the size of bamboo leaf, the microwave is scattered at a canopy of a bamboo as shown in Figure 3(a). On the other hand, the wavelength of L band microwave is larger than a size of a bamboo leaf, and the microwave penetrates a bamboo as shown in Figure 3(b).

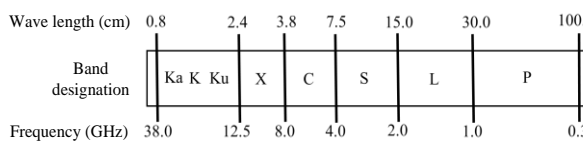


Figure 2: Radio spectrum of radar-wavelength band.

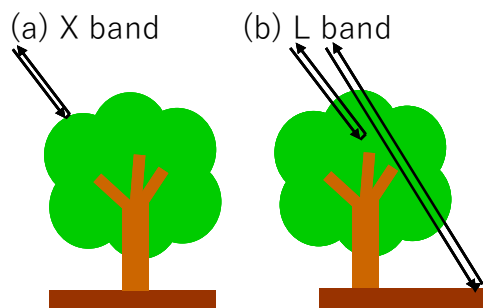


Figure 3: Difference of scattering properties to vegetation by wavelength. (a) X band is scattered at canopy, (b) L band is scattered at internal forest or earth surface.

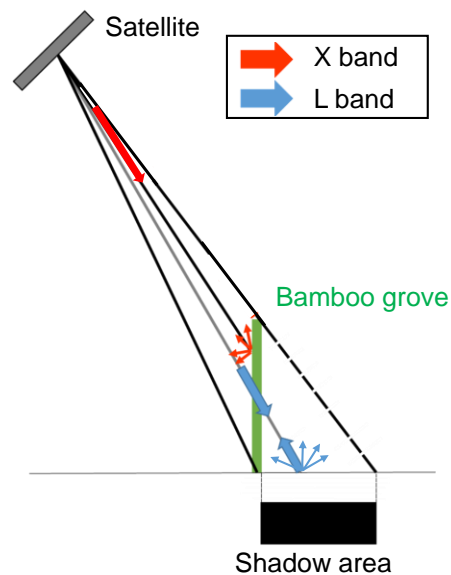


Figure 4: Difference of penetration to a bamboo grove between L and X band microwave.

2.2 Difference of vegetation imaging between L and X band SAR images

The difference of reflection-scattering properties between L and X band microwaves affects backscattering observed in SAR images. While L band microwave penetrates a bamboo grove, X band microwave is scattered by a bamboo grove as shown in Figure 4. Hence, L band SAR observes scattering from earth surface behind a bamboo grove on a line-of-sight of a satellite, but X band SAR does not observe backscattering behind a bamboo grove. Therefore, we assumed that shadow areas were observed only in an X band SAR image.

2.3 Image modulation of SAR image

We describe image modulation of SAR image to develop a vegetation height estimation method.

In SAR imagery, a distance between a satellite and a scattered object affects map projection. On undulating ground, the top of a scattered object is projected closer to a satellite than actual position as shown in Figure 5 (a), because the distance from the top to the satellite is shorter than that from the foot. This phenomenon is called ‘foreshortening’. A satellite cannot observe behind a scatterer as shown in Figure 5 (a), and this is known as ‘shadowing effect’. We observe shadow areas behind a bamboo grove only in X band SAR image due to foreshortening and shadowing effects.

2.4 Estimation equation of vegetation height by L and X band SAR images

We proposed a method to estimate heights of vegetation in riverine areas using the difference of the reflection-scattering properties based on image modulation of SAR image.

Figure 5(b) shows relationship between length of a shadow area and height of a scatterer. The length of shadow area is denoted by:

$$l_s = h \tan \theta, \quad (1)$$

where θ is incidence angle (Soergel et al., 2009, Ouchi 2009). A scatterer is assumed a line object.

As shown in Figure 5(c), relationship between foreshortening length δl with height of scatterer is denoted by:

$$\delta l = h \cot \theta. \quad (2)$$

Here, we use an approximation

$$R \cong R_0 - h \cos \theta. \quad (3)$$

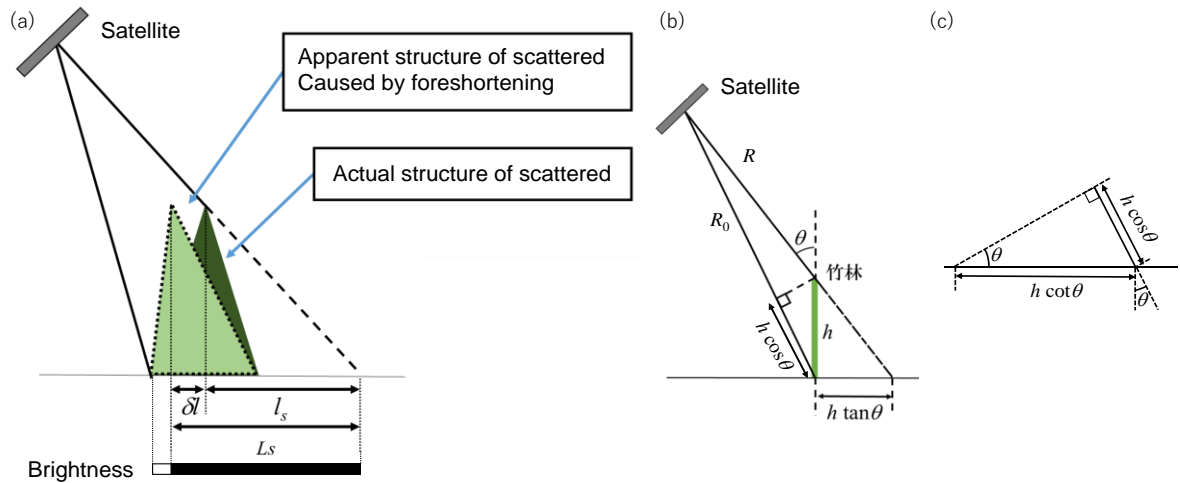


Figure 5: (a) Geometric image modulation in SAR image. The gap of scatterer top caused by foreshortening is δl . Length of shadow area caused by shadowing effect is l_s . Total length of shadow area is L_s . (b) Length of shadow area l_s is denoted by $l_s = h \tan \theta$, where θ is incidence angle. (c) Foreshortening length δl is denoted by $\delta l = h \cot \theta$.

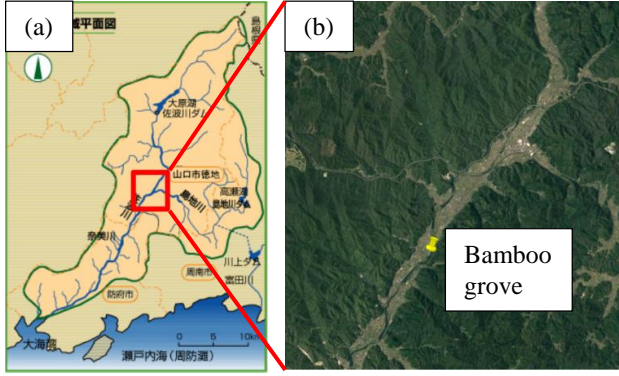


Figure 6: (a) Saba River Basin (MLTI 2016), (b) Aerial shooting area.

Table 1: The schedule of SAR satellite image and drone aerial shootings.

Date (2016)	Action
Sep. 14	L band SAR image shooting
Oct. 7	Drone aerial shooting
Nov. 8	X band SAR image shooting

As shown in Figure 5 (b), where R is a distance between a satellite and the top of a bamboo grove, R_0 is a distance between a satellite and the bottom of a bamboo grove. Since the satellite and the ground are extremely far away, the line between the satellite and the top of a bamboo grove and the line between the satellite and the bottom of a bamboo grove are assumed to be parallel, then Eq(3) holds.

Projecting the difference of distance $h\cos\theta$ to the ground, we obtain foreshortening length Eq(2) as shown in Figure 5 (c). Thus, total shadow length in SAR image L_s is the sum of l_s and δ as shown in the following:

$$L_s = l_s + \delta l = h \tan \theta + h \cot \theta . \quad (4)$$

From Eq.(4), we obtain

$$h = L_s / (\tan \theta + \cot \theta) . \quad (5)$$

Eq.(5) is the equation that we proposed estimating vegetation heights.

3. ACCURACY VERIFICATION

3.1 Ground measurement of vegetation height by drone aerial shooting

To obtain ground truth data, we measured vegetation height by drone aerial shooting. We produced a 3D model by structure from motion (SfM) analysis of aerial photos, and vegetation heights were obtained from the 3D model.

Figure 7 (a) and (b) show the the Saba River Basin and the ground measurement area by drone aerial shooting, respectively (MLTI 2016). The aerial shooting area is located 19.9 km from the river mouth where bamboos grow on the riverbank. Table 1 shows the schedule of SAR satellite image and drone aerial shootings. We used the SAR images that are shoot within about a month from drone aerial shooting so that we can assume the state of vegetation had not changed so much.

3.2 Comparison of drone aerial shooting with SAR images

Figure 7 shows (a)orthophoto, (b) vegetation canopy heights measured by drone aerial shooting, (c) L band SAR image (ALOS2/PALSAR-2), and (d) X band SAR image (TerraSAR-X) at the study area. As shown in Figure 7 (a) and (b), the heights of bamboo groves on the right bank are around 10 meters. Brightness of SAR images, Figure 7 (c) and (d), correspond with backscattering intensity. A bright area corresponds with high intensity, and a dark area corresponds with low intensity, respectively. In the framed area in Figure 7(b), a bamboo grove was cutover after drone aerial shooting. We measured the heights of the two cutover bamboos, and they are 9.5m and 11.0 meters. This verified that the drone aerial shooting measured bamboo canopy heights accurately. Comparing Figure 7 (c) and (d), while we observed clear shadow areas behind bamboo groves on the line-of-sight of the satellite in the X band SAR image, any distinctive shadow area was not observed in the L band SAR image.

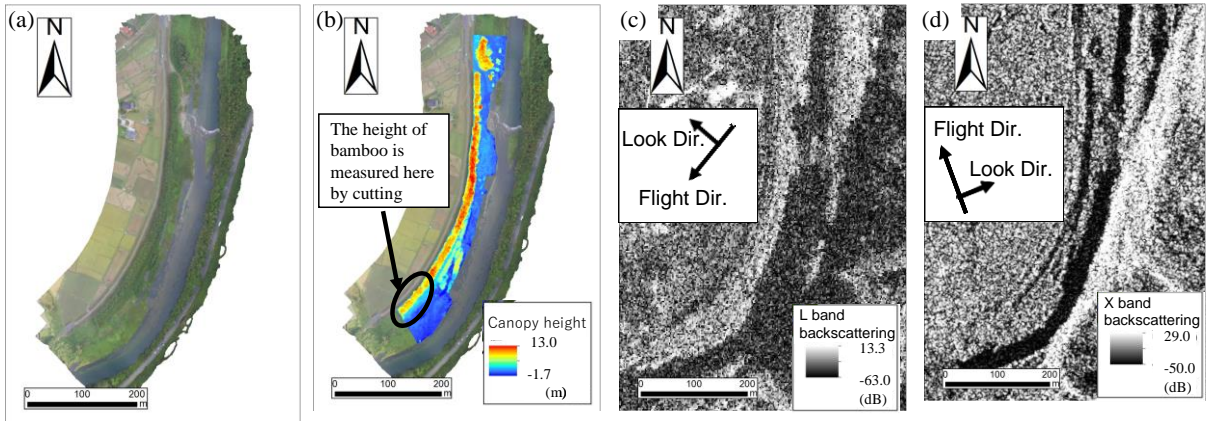


Figure 7: Study area. (a) Orthophoto, (b) vegetation canopy height, (c) L band SAR image, and (d) X band SAR image.

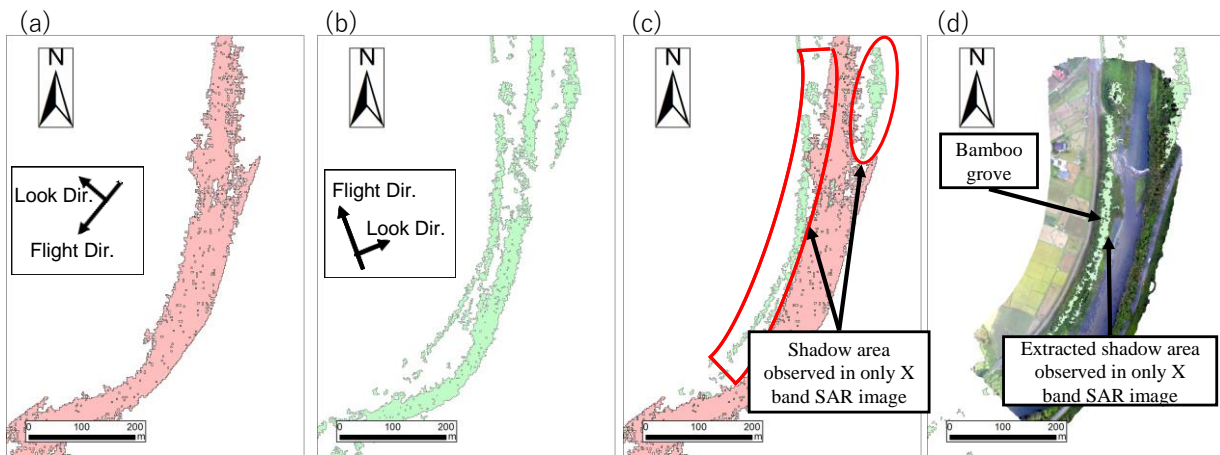


Figure 8: The shadow area where the backscattering coefficient is less than threshold value (a) in L band SAR image, (b) in X band SAR image. (c) Overlay of shadow areas of L and X band. Framed areas are shadow areas observed in only X band. (d) Overlay of extracted shadow area observed in only X band and the orthophoto.

3.3 Differential extraction of L and X band SAR image and comparison with the bamboo grove area

As shown in Figure 7 (c) and (d), clear shadow areas were observed along the bamboo groves only in X band SAR image. Using this result, we detected a bamboo grove by differential extraction of L and X band SAR images. The shadow area where the backscattering coefficient values were less than the threshold value is extracted for L and X band SAR images as shown in Figure 8 (a) and (b). The threshold values were determined by referring the backscattering coefficient value of water surface, where backscattering was low due to high absorption of microwave to water. The threshold of L band was -13.5 dB and X band was -15.0 dB. Figure 8 (c) shows the overlay of shadow areas in L and X band, and the framed area was the shadow area observed only in X band SAR. Removing L band shadow area from X band shadow area, we obtained the shadow area observed only in X band SAR as shown in Figure 8 (d). The shadow area observed only in X band SAR exists along a bamboo grove. Thus we detected bamboo groves by differential extraction of L and X band SAR images.

3.4 Accuracy verification of proposed equation for estimation of vegetation height

The length of extracted shadow area L_s is obtained as shown in Figure 9. The vegetation height h is estimated by substituting L_s into Eq(5). The accuracy of proposed estimation equation is verified by comparison with measured vegetation height by drone aerial shooting.

A calculation example is shown in the following. The shadow length shown in Figure 9 is measured as $L_s=15.4$ m, the incidence angle θ is 41.0 degree. Substituting these values into Eq(5), we have

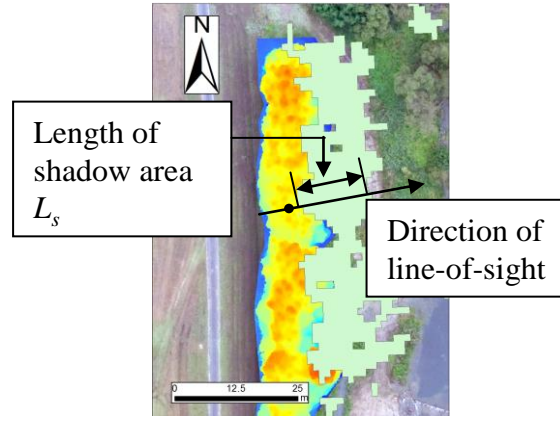


Figure 9: Measuring the length of the shadows observed in only X band SAR image.

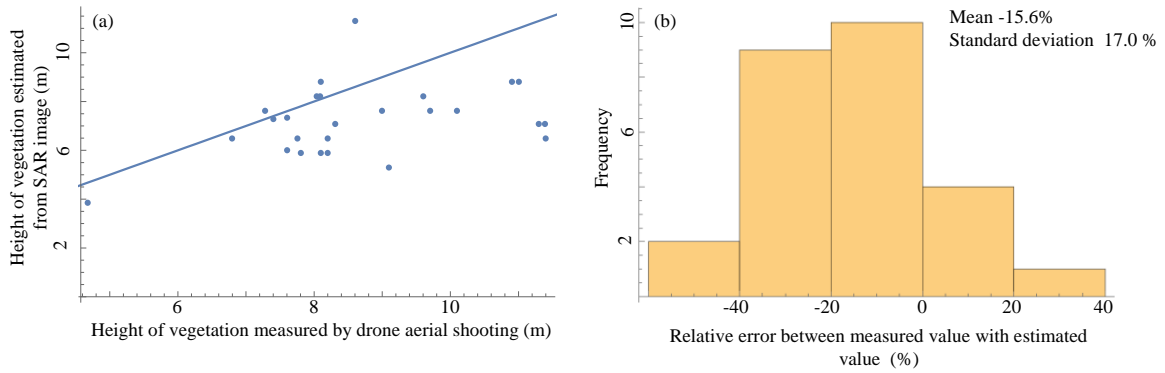


Figure 10: (a) The scatterplot of vegetation height between measured value with estimated value. (b) The histogram of the relative error between measured value with estimated value of vegetation height.

$$h = L_s / (\tan \theta + \cot \theta) = 15.4 / (\tan 41^\circ + \cot 41^\circ) = 7.63 \text{ (m)}. \quad (6)$$

The vegetation height measured by drone aerial shooting is 7.28 m.

In the same way, the vegetation height values estimated by substituting shadow length L_s into Eq(5) are compared with measured vegetation height values by drone aerial shooting at 27 points. Figure 10 (a) shows the scatter plot of vegetation height between measured value with estimated value. Figure 10 (b) shows the histogram of the relative errors between measured value and estimated value. The mean and standard deviation of the relative errors are -15.6 %, 17.0 %, respectively. This result suggests that while the proposed method for vegetation height estimation cannot provide accuracy of several tens cm to 2 meters, it has a potential to measure vegetation heights roughly.

Horizontal resolution of SAR image also affects the accuracy of vegetation height estimation. The horizontal resolution of SAR images used in this study is 3 meters, and it is natural that the same degree errors with resolution are observed.

3.5 Limitation of the proposed method

As shown in Figure 8 (c), while bamboo groves on the right bank were detected accurately, bamboo groves on the left bank was not observed by differential extraction of L and X band SAR images. There are mountains on the left side of the river. Since the mountains were projected to the riverine area by foreshortening, the bamboo groves on the right bank was not observed in X band SAR image.

Direction of bamboo groves affects vegetation detection by SAR. In case of directions of bamboo groves and the line-of-site of a satellite are nearly orthogonal, bamboo groves were detected by differential extraction of L and X band SAR images as shown in Figure 8. However, in case of the directions are nearly parallel, bamboo groves were not detected well as shown in Figure 11.

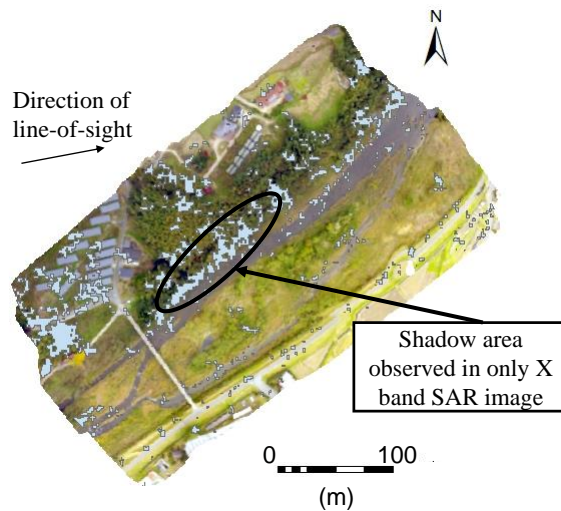


Figure 11: An orthophoto and extracted shadow area where river flow is nearly parallel to direction of line-of-site. Thus, foreshortening effect caused by high objects, such as mountains, and direction of vegetation line against the line-of-site of a satellite constrain the proposed method.

4. CONCLUSION

We applied SAR satellite imaging to vegetation monitoring in the Saba River in Japan. Results are as follows:

- We developed a method to estimate bamboo heights by using SAR image based on the difference of reflection-scattering properties between L and X band microwaves. We demonstrated that the shadow areas observed only in X band SAR was along bamboo groves in the Saba River.
- We proposed an equation to estimate a bamboo height from a length of a shadow area based on image modulations of SAR. We verified the accuracy of the proposed equation comparing with bamboo heights measured by drone aerial shooting. The mean and standard deviation of relative errors between the estimated and measured values were -15.6 %, 17.0 %, respectively.
- The method was affected by terrain condition, vegetation line direction, and line-of-site of a satellites. In case of vegetation line direction was parallel to line-of-site direction, the shadow area observed only in X band SAR did not detect vegetation well. Mountains near the river also causes SAR image modulation and makes difficult to estimate vegetation height.

Using the difference of reflection-scattering properties of L and X band microwaves, we proposed vegetation observation method. The method is expected to contribute to effective and efficient river vegetation monitoring and reducing flood risks .

References:

- Japan Aerospace Exploration Agency (JAXA), 2016. Data Release of Global Forest/Non-forest Map by DAICHI-2-Contributing to measures to tackle global warming by understanding forest areas -, Retrieved August 24, 2017, from http://global.jaxa.jp/press/2016/01/20160128_daichi2.html
- Ministry of Land, Infrastructure, Transport and Tourism (MLTI), Chugoku Regional Development Bureau, Yamaguchi Office of River and National Highway, 2016. Retrieved August 24, 2017, from <http://www.cgr.mlit.go.jp/yamaguchi/river/school/01.html>
- Okamoto, T. et al. 2013. Experimental study on diverging flow at the boundary between flat bed zone and vegetation patch zone, journal of japan society of civil engineers, ser. b1 (hydraulic engineering), vol. 69, No. 4, pp. I_871-I_876.
- Ouchi, K., 2009. Principles of synthetic aperture radar for remote sensing, Tokyo Denki University Press, Tokyo, pp. 123-130.
- Partama, I. GD. Y. et al., 2016. Preliminary study on monitoring vegetation height using L-band ALOS/PALSAR-2 data in river scale, the Remote Sensing Society of Japan, p.37.
- Sanuki, S. et al. 2010. The present state of development of thck growth of trees. and vegetation management in class a rivers, Advances in river engineering, vol. 16, pp. 241-246.
- Sasaki, S. et al. 2017, The development of a vegetation monitoring method in Japanese rivers using synthetic aperture radar(SAR), Journal of Japan Society of Civil Engineers, Ser. G (Environmental Research), Vol. 73, No. 5, I_303-I_308(in Japanese).

Shige-eda, M. et al., 2006. Flood simulations in the ototsu river with vegetations by a two-dimensional numerical model, Proceedings of hydraulic engineering, vol. 50, pp. 1171-1176.

Shimizu, Y. et al. 2006. Numerical simulation of the driftwoods behavior by using a dem-flow coupling model, Proceedings of hydraulic engineering, vol. 50, pp. 787-792.

Soergel, U. et al.,2009. Stereo analysis of high-resolution SAR images for building height estimation in cases of orthogonal aspect directions, ISPRS Journal of Photogrammetry and Remote Sensing 64, 490–500.